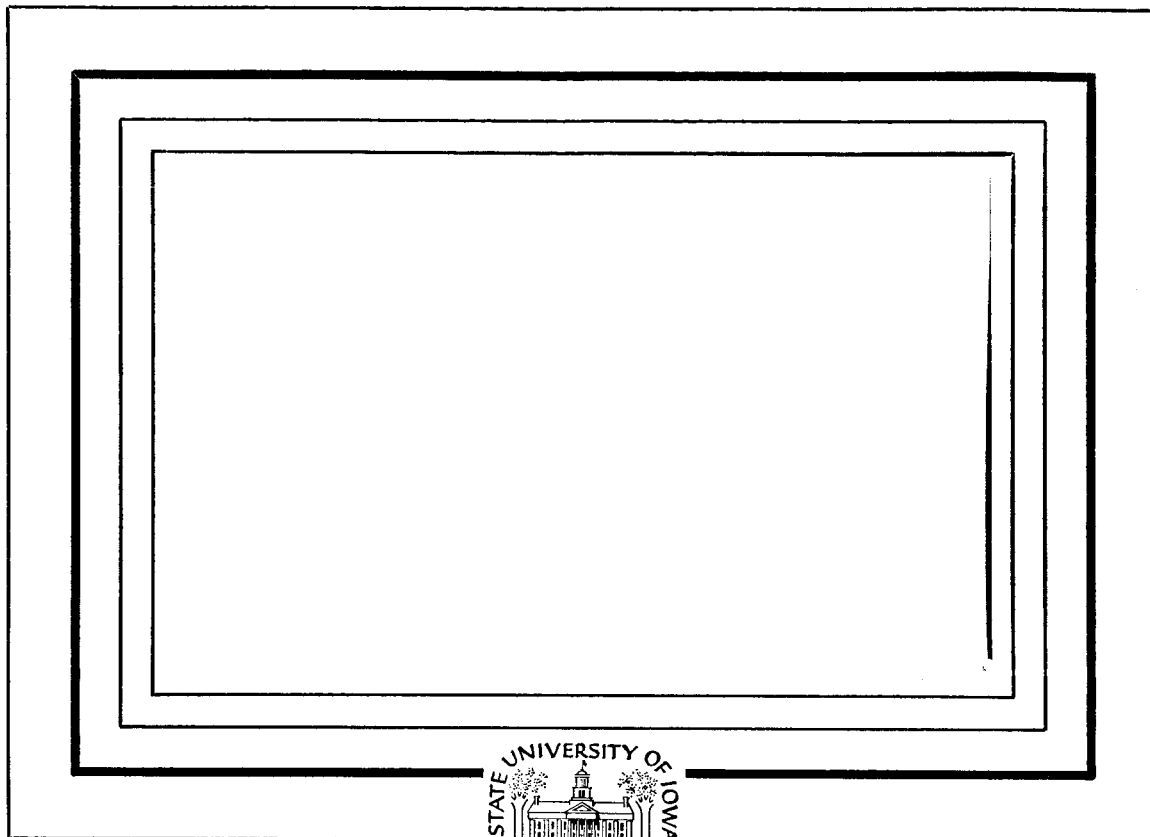


U. of Iowa 65-3

UNPUBLISHED PRELIMINARY DATA

~~SECRET~~



841

N65-25004  
(ACCESSION NUMBER)

60  
(PAGES)

CR 62893  
(NASA CR OR TMX OR AD NUMBER)

(THRU)

1  
(CODE)

29  
(CATEGORY)

GPO PRICE \$ \_\_\_\_\_

OTS PRICE(S) \$ \_\_\_\_\_

Hard copy (HC) 3.00

Microfiche (MF) .50

Department of Physics and Astronomy  
STATE UNIVERSITY OF IOWA

Iowa City, Iowa

FACILITY FORM 602

Diurnal and Latitude Effects Observed for  
10 keV Electrons at Low Satellite Altitudes\*

by

Theodore A. Fritz and Donald A. Gurnett<sup>+</sup>

February 1965

Department of Physics and Astronomy  
University of Iowa  
Iowa City, Iowa

\*This work was supported in part by the Office of Naval Research under contract Nonr 1509(06) and by the National Aeronautics and Space Administration under grant NSG-233-62.

<sup>+</sup>Graduate Trainee of the National Aeronautics and Space Administration.

## ABSTRACT

25004

Using a low energy electron detector on the low altitude, high latitude satellite Injun III, large diurnal and latitude effects have been observed for 10 keV electrons. It is found that intense fluxes of low energy electrons,  $j(E_e \geq 10 \text{ keV}) \geq 2.5 \times 10^7$  electrons  $(\text{cm}^2 \text{ ster sec})^{-1}$ , occur only during local night between 1700 hours and 0700 hours (magnetic local time) and that they occur only between  $58^\circ$  and  $76^\circ$  invariant latitude. These intense fluxes of low energy electrons occur predominantly during periods of high geomagnetic activity. It is also found that a large change in the slope of the electron energy spectrum is associated with the trapping boundary for 40 keV electrons found at high latitudes during local night. This change is from a relatively hard spectrum inside the boundary to a very soft spectrum just outside the boundary. The intense fluxes of very soft electrons found beyond the 40 keV trapping boundary at low altitudes are thought to be related to the intense fluxes of low energy electrons found by Gringauz and by Freeman at great distances on the night side of the earth.

Author

## INTRODUCTION

The existence of intense fluxes of low energy ( $E_e < 40$  keV) electrons in and near the outer Van Allen trapping region has been established by a number of experimenters. The first direct observation of these electrons was made by balloon-launched rockets in 1952 by Van Allen [1957] and the Iowa group. Fuller studies of electrons within visible auroras with rockets were made by Meredith et al. [1958], McIlwain [1960], and McDiarmid et al. [1961 and 1964a]. Krasovskii et al. [1962], O'Brien and Laughlin [1962], Gringauz et al. [1962], Sharp et al. [1964 a and b], and Freeman [1964] have reported measurements made on such electrons with satellite-borne experiments. The measurements of Krasovskii et al. [1962], O'Brien and Laughlin [1962], and Sharp et al. [1964 a and b] were made at low altitudes on near polar orbiting satellites. Their reported maximum energy fluxes of  $360 \text{ ergs (cm}^2 \text{ sec ster)}^{-1}$  (with  $\bar{E}_e = 10$  keV);  $400 \text{ ergs (cm}^2 \text{ sec ster)}^{-1}$  ( $E_e \geq 1$  keV); and  $100 \text{ ergs (cm}^2 \text{ sec ster)}^{-1}$  ( $E_e \geq 2$  keV), respectively, are in good agreement with one another. Freeman [1964], using Explorer 12 data, reported the existence of a large flux of soft electrons on the night side near the geomagnetic equator outside the trapping boundary for 40 keV electrons

in the outer Van Allen belt. These fluxes were of the order of  $\sim 10^9$  electrons  $(\text{cm}^2 \text{ sec ster})^{-1}$  for an assumed average electron energy of 10 keV. These results are in general agreement with those of Gringauz et al. [1962] who found a similar region of low energy electrons on a single traversal of this region with the Lunik 2 space probe.

It is the purpose of this paper to report the results obtained with a low energy electron ( $E_e \geq 10$  keV) detector flown on the low-altitude, high latitude satellite, Injun 3. The ONR/U. of Iowa satellite Injun 3 was launched on December 13, 1962 into an orbit with initial apogee altitude 2785 km, perigee altitude 237 km, orbital inclination  $70.4^\circ$ , and period 116 min [O'Brien, Laughlin, and Garnett, 1964].

## DESCRIPTION OF THE ELECTRON MULTIPLIER

The Electron Multiplier was constructed and calibrated by D. E. Stilwell. The details of this work are unpublished but are documented in State University of Iowa Research Report 63-28 [Stilwell, 1963]. The Electron Multiplier consisted of a multiplier structure similar to that of a conventional photomultiplier. Incident particles, striking the sensitive area of the first dynode directly produced electrons by a secondary emission process. These secondaries were drawn on to successive dynodes by an accelerating potential, thus providing current multiplication. The resulting anode current was proportional to the incident particle number flux and this current was fed to a simple neon-glow tube relaxation oscillator whose output frequency was a function of the current drawn from the circuit input. In this manner an analog to digital conversion of the anode current was accomplished [Stilwell, 1963].

The Electron Multiplier on Injun 3 was a 19 stage Venetian blind structure modified from an Ascop 541 series photomultiplier tube. The dynode material was Ag (MgO) with 2500 volts applied to the dynode voltage divider resistors. The minimal design gain of the tube was to be  $\sim 5 \times 10^6$  at this applied voltage [Stilwell, 1963]. Stilwell, upon

calibrating the detector, found the gain to be  $2.5 \times 10^5$  and he attributed this difference to an absorbed monolayer of atmospheric gases on the dynode surfaces. The aperture of the Electron Multiplier was covered by a thin ( $86 \mu\text{g}/\text{cm}^2$ ) nickel foil which served two purposes. First, the presence of the foil minimized false signals due to ultra-violet and visible radiation from the sun. Second, it was deemed desirable to make the energy threshold of the Electron Multiplier identical to that of another detector, the D. C. Scintillator, for which the foil was necessary in order to protect it from damage due to sunlight. The absolute calibrations of this companion detector later proved to be untrustworthy in flight. The foil imposed a threshold on the multiplier of approximately 10 keV for electrons. Stilwell [1963] has given a response function for the Electron Multiplier based on the preflight calibrations he performed (upper curve in Figure 3). In his post-launch calibration checks, he was able to determine that the foil had survived the first six months of satellite operation and he stated that the gain had remained constant to within  $\sim 10\%$  over this same period. These checks were made by noting the detector response to sunlight. As for the post-launch check on the absolute gain of the multiplier, Stilwell

was able to say that no reason had arisen to doubt the preflight calibration of this parameter.

On Injun 3, which was magnetically oriented, detector orientations were referenced by the angle  $\theta$  between the axis of the detector and the satellite's magnetic axis. When the satellite was properly aligned, the  $\theta = 0^\circ$  axis was parallel to the geomagnetic B-vector and was directed down into the atmosphere in the Northern Hemisphere. The Electron Multiplier was in the  $\theta = 130^\circ$  position and measured particles which had a pitch-angle (the angle the particle's velocity vector makes with the geomagnetic B-vector) of  $50^\circ \pm 10^\circ$  when the satellite was properly oriented [O'Brien, Laughlin, and Gurnett, 1964]. The orientation of the satellite was measured with two Schonstedt flux gate magnetometers mounted with their axes parallel to  $\theta = 90^\circ$  and  $\theta = 130^\circ$ , respectively.



INFLIGHT CALIBRATION OF THE  
ELECTRON MULTIPLIER

The purpose of this subsidiary investigation was twofold:

(1) It was desired to establish the absolute sensitivity of the Electron Multiplier using data recorded while the satellite was in flight and once this sensitivity had been found, (2) it was desired to see if the gain of the Electron Multiplier had remained approximately constant throughout the life of the satellite.

Since no other detector aboard Injun 3 was sensitive to low energy electrons ( $E_e \ll 40$  keV), it was necessary to make some assumption regarding the electron energy spectrum between 10 keV and 40 keV. For this reason, the calibration points were taken in a region of the inner zone because the electron fluxes there are relatively stable and their energy spectrum is relatively hard compared to that of the outer zone electrons [O'Brien, 1963].

Since the Electron Multiplier can respond to particles through a secondary emission process or photons through a photo-electric process, it was first necessary to investigate whether the multiplier was responding to particles or to light or x-rays while in the inner zone. Since the satellite

was equipped with an optical aspect sensor which "locked" in the same direction as the multiplier, all data taken when the sun was in the multiplier's viewing cone could be eliminated.

Frank [1962] and Laughlin [1960] have investigated the counting rate of Geiger tubes due to x-rays produced by particle bombardment of the satellite shell. Frank, using a 302-type Geiger tube, has shown that the maximum possible variation in the counting rate due to the extremes in particle angular distributions bombarding a spherical Injun 3-type shell was less than a factor of two. The actual angular distribution of particles seen by Injun 3 would make this variation even smaller. Since the particle flux in the inner zone is known to be peaked at a pitch angle of  $90^\circ$ , it is argued that if the counting rate of the Electron Multiplier exhibited a definite angular distribution peaked at a pitch angle of  $90^\circ$ , then it was indeed responding to particles. This argument was strengthened by observing the response of the heavily shielded SpB detector on Injun 3, which was primarily due to bremsstrahlung and to penetrating protons. This response varied monotonically and was independent of the satellite's orientation. Four such distributions are shown in Figure 1, where a comparison can be made between the Electron Multiplier response and the SpB response. Figure 1 demonstrates that the Electron Multiplier was responding to particles in the inner zone and not to x-rays.

In order to calibrate the Electron Multiplier's response to these particles, a simple spectral form was chosen and a proper fit was made using the rates of the various detectors on the satellite. In the literature the two popular spectral forms are the exponential ( $dN = N_0 e^{-E/E_0} dE$ ) and the power law ( $dN = KE^{-\gamma} dE$ ). Although only a rough approximation, the exponential spectral form has been shown to give a fairly good spectral fit for portions of the electron energy spectrum in certain regions of the inner zone [West, Bloom, and Mann, 1964; Pizzella et al., 1964]. On Injun 3 in the  $\theta = 130^\circ$  position, there were no detectors from which spectral information could be obtained.

In the  $\theta = 90^\circ$  position, there were four detectors which could be used to determine the electron energy spectrum [O'Brien, Laughlin, and Gurnett, 1964]. Detector 1 was a thin windowed directional 213-type Geiger tube with an angular field of view of about  $26^\circ$  diameter and a window thickness of  $1.2 \text{ mg cm}^{-2}$  of mica. It had an energy threshold for electrons of approximately 40 keV. Detector 3 was similar to detector 1 but had an additional window thickness of  $45 \text{ mg cm}^{-2}$  of aluminum, which gave this detector an energy threshold of approximately 250 keV for electrons. The other two detectors

were the SpL and SpH channels of the magnetic differential electron spectrometer. These detectors were also 213-type Geiger tubes which were encased in a lead cylinder  $3.5 \text{ g cm}^{-2}$  thick. Two magnets bent electrons into SpL and SpH with energy  $E_e$  such that  $40 \text{ keV} \lesssim E_e \lesssim 55 \text{ keV}$  for SpL and  $80 \text{ keV} \lesssim E_e \lesssim 100 \text{ keV}$  for SpH. A third 213-type Geiger tube (SpB) encased in the lead cylinder measured the omnidirectional intensity of penetrating particles and bremsstrahlung and thereby permitted a background correction to be made to the above four detectors.

Because of the large fluxes present in the inner zone where these calibrations were made, detector 1 was operating far into the non-linear region of its apparent rate versus true rate curve. Due to uncertainties in this curve [O'Brien, Laughlin, and Gurnett, 1964], it was decided not to rely on detector 1 in any manner for this calibration.

Early in the life of Injun 3, while the satellite was tumbling, detectors in the  $\theta = 90^\circ$  position and the Electron Multiplier ( $\theta = 130^\circ$ ) measured particles with various pitch angles. At certain times the pitch angle of the particles measured by the detectors at  $\theta = 90^\circ$  was identical to the pitch angle of particles measured by the Electron Multiplier.

At these times, using the responses of SpL and detector 3 corrected for background, a two parameter exponential type spectrum ( $dN = N_0 e^{-E/E_0} dE$ ) was fitted for the energy range between 40 keV and 250 keV. As a further refinement, the validity of this fit was checked by comparing the actual response of the SpH channel with that predicted by the spectrum. A spectral fit was used as a calibration check only if the predicted and measured response of SpH agreed to within  $\pm 40\%$ . (75% of the calibration points actually agreed to better than  $\pm 15\%$ .) Table I is a list of the calibration points used in this investigation. Figure 2 is a graph of the results of the inflight calibration of the multiplier and these results can be compared with the preflight calibrations made by Stilwell [1963]. The preflight calibrations were performed up to an electron energy of approximately 90 keV. The response of the detector for energies above 90 keV was unknown but according to Bruining [1954] the response function was probably constant to a first approximation for  $E_e \gg 90$  keV up to at least 300 keV [see Bruining, page 47]. In Figure 3, three assumed forms (A, B, and C) of the high energy portion of the response function are shown. Curve B was the response function chosen for evaluating the data. The lower curve in

Figure 3 is the final result of the inflight calibration of the absolute sensitivity of the Electron Multiplier.

In the  $\theta = 130^\circ$  position there were two detectors in addition to the Electron Multiplier which were sensitive to direct sunlight [O'Brien, Laughlin, and Gurnett, 1964]. The optical aspect sensor was a "yes-no" device telling when the sun was in its viewing cone, and the D. C. Scintillator, although proving untrustworthy as a calibrated detector, was very sensitive to sunlight. Using these two detectors and the various particle detectors on the satellite, it was possible to tell when the Electron Multiplier was "looking" directly at the sun and at the same time had only a negligible particle response. Responses of this kind were tabulated throughout the life of the satellite and the maximum responses during each revolution are presented in Figure 4. The responses are grouped in three time periods because of favorable satellite orientation during these periods. From Figure 4 we infer that the foil survived the entire useful lifetime of the satellite and that the gain had remained constant over the same period. This is in agreement with the earlier calibration checks made by Stilwell [1963].

It is now necessary to examine the accuracy of the above described calibration procedure. There are three major areas in which error could occur. The first area is the assumption that an exponential spectrum fitted to the data between electron energies of 40 keV and 250 keV is valid for electron energies down to 10 keV. The second area is concerned with the error present in the determination of the spectral parameters. This area includes the stated error in the response functions of the various detectors, statistical errors in the detector counting rates, and error due to background corrections. The last area is concerned with the possible error incurred in the assumption of the high-energy portion of the response function for the Electron Multiplier. We will now investigate each of these areas individually.

The assumption that the electron energy spectrum between 10 keV and 40 keV can be reasonably predicted by a knowledge of the spectrum between 40 keV and 250 keV is the major assumption in this calibration procedure. It was for this reason that reasonably "hard" spectra were chosen as calibration points since there is very little low energy electron spectral information in the literature. For these "hard" spectra, the exponential spectral form we have chosen predicts that approximately 75% of

the electrons with  $E_e \geq 10$  keV (measured by the Electron Multiplier) have  $E_e \geq 40$  keV and are measured by other detectors on the satellite. Therefore, regardless of the spectral form below 40 keV, this calibration procedure sets a lower limit on the electron fluxes measured by the Electron Multiplier. We believe that this procedure is the best approach to the problem but there is no way of attaching a meaningful, quantitative error to this assumption.

The spectral parameters were determined from the following ratio:

$$\text{Ratio} = \frac{\left( R_{\text{SpL}} - (G_{\text{SpL}}/G_{\text{SpB}}) R_{\text{SpB}} \right) \epsilon_{\text{Det. 3}} (E_e)}{\left( R_{\text{Det. 3}} - (G_{\text{Det. 3}}/G_{\text{SpB}}) R_{\text{SpB}} \right) \epsilon_{\text{SpL}} (E_e)}$$

- where  $R_i$  = counting rate of the given detector  
 $G_i$  = omnidirectional geometric factor  
 $\epsilon_i$  = unidirectional geometric factor

The value of the ratio,  $G_i/G_{\text{SpB}}$ , was determined from cosmic ray background and was checked using cases where the detector response was due entirely to penetrating radiation in the inner zone. The relationship between the spectral parameters and the ratio was determined by a numerical integration of the response functions for various exponential spectra. The stated error



in the response function  $\epsilon_{SpL}(E_e)$  is  $\pm 20\% \sqrt{C}$ . D. Laughlin, private communication. We assumed a similar error for  $\epsilon_{Det. 3}(E_e)$ . In order to avoid excessive uncertainties due to background corrections, data were used only if the following conditions were met:

$$\left( R_{SpL} - (G_{SpL}/G_{SpB}) R_{SpB} \right) \geq 0.5 R_{SpL}$$

$$\left( R_{Det. 3} - (G_{Det. 3}/G_{SpB}) R_{SpB} \right) \geq 0.9 R_{Det. 3}$$

With these restrictions and the possible errors present in the omnidirectional geometric factor ratios, the statistical errors (assuming  $R_1$  is a Poissonian variable), and the stated error in the response functions, we believe each ratio calculated is accurate to  $\pm 29\%$ . This error is due mostly to the stated error in the response functions for SpL and detector 3 and not to statistical errors in the data. To illustrate this fact the standard deviation in the mean of the 12 ratios used in this procedure was 2.6%.

In investigating possible error due to the assumption of the high energy portion of the response function for the Electron Multiplier, we are again faced with the difficulty of assigning a meaningful, quantitative error. As an estimate, we consider

the difference between the limiting forms of curve A and curve C in Figure 3. This would lead to an error of approximately  $\pm 20\%$  in the calibration of the response function for the Electron Multiplier.

By combining the errors stated above we arrive at an estimate of  $\pm 35\%$  for the probable error in the absolute response function for the Electron Multiplier, without taking into account any error due to the assumption of a spectral form in the calibration.

As a result of these inflight calibrations and the preflight calibrations performed by Stilwell [1963], the response of the Electron Multiplier was found to be linear from  $10^2$  counts/second down to at least  $2 \times 10^{-2}$  counts/second. The latter value is taken as the threshold rate for the Electron Multiplier.

## THE STUDY

Since the satellite traveled a distance of 6 to 7 km in one second and the particle flux could change drastically over the wide region between multiplier threshold responses, a restriction that the counting rate be equal to or greater than 0.12 count/second was imposed on this study. This exact figure was chosen because of the ease with which it could be recognized in the data format. For a relatively soft electron spectrum ( $3.0 \text{ keV} \leq E_0 \leq 20 \text{ keV}$  where  $dN = N_0 e^{-E/E_0} dE$ ), this counting rate corresponds approximately to  $j(E_e \geq 10 \text{ keV}) \approx 2.5 \times 10^7$  electrons  $(\text{cm}^2 \text{ sec ster})^{-1}$ . It is pointed out here that the Electron Multiplier was equally sensitive to protons with  $E_p \geq 50 \text{ keV}$  and the assumption made throughout this paper that the Electron Multiplier was responding only to electrons with  $E_e \geq 10 \text{ keV}$  cannot be proved. Plausibility arguments in favor of this assumption however will be given in Appendix II.

A complete tabulation of all Electron Multiplier responses for  $L \geq 2.0$  ( $L$  is the geomagnetic shell parameter of McIlwain [1961]) was made for the entire 10 months of Injun 3 data. On every occasion when the Electron Multiplier response equaled or exceeded 0.12 count/second the response was labeled in one of

three ways: (1) Response due to direct sunlight, (2) response due to a large flux of electrons, i.e., a valid event, and (3) noisy or bad telemetry.

The light responses were easily distinguished from the responses due to particles by using the solar aspect sensor and the D. C. Scintillator. For a light response, the solar aspect gave a "yes" reading indicating that the sun was in its viewing cone and the D. C. Scintillator's counting rate was  $10^3$  to  $1.5 \times 10^3$  counts/second. For a valid particle event, the solar aspect gave a "no" reading and the D. C. Scintillator rate never exceeded 80 counts/second and was usually  $\sim 15$  counts/second. This latter rate is two orders of magnitude below the rate due to direct sunlight. In only two cases was it believed that the Electron Multiplier might be responding to light and to particles simultaneously. These two cases were classified as light responses in this study.

The criteria for the elimination of data due to noise and bad telemetry were rather subjective and were based on past experience with the data. It was the purpose of this study to make the final sample as trustworthy as possible. Of the 1191 responses of the Electron Multiplier which were equal to or greater than 0.12 count/second, 622 were labeled as valid

particle responses, 426 as due to light and 143 as due to noise. The small amount of data ( ~ 12%) eliminated as due to noise was found to be randomly distributed in any sample of Injun 3 data and therefore did not affect the results of this study.

## RELEVANT PARAMETERS

In order to investigate diurnal or latitude effects a set of relevant coordinates must be chosen in which to organize the data. To display the data in this paper we have chosen the 'invariant latitude',  $\Lambda$ , and 'magnetic local time' as the parameters of interest.

The invariant latitude  $\Lambda$  [O'Brien, 1962] is derived simply from the L coordinate of McIlwain [1961] by the relation

$$L \cos^2 \Lambda = 1 .$$

This parameter is used here because the L parameter is found to be very useful in introducing order into studies of trapped particles and because it is derived from a much higher-order expression for (and therefore a more accurate description of) the geomagnetic field than is the usual expression for magnetic latitude [O'Brien and Taylor, 1964]. The invariant latitude  $\Lambda$  differs from the geomagnetic latitude generally by less than  $2^\circ$  over North America where most of the data in this study were taken [O'Brien, 1962].

Magnetic local time is defined as the angle between the planes which are defined by the geomagnetic dipole axis and the earth-sun line and by the geomagnetic dipole axis and the earth-

center-satellite line. (For further remarks on magnetic local time, see Appendix I.) Magnetic local time takes into account both the daily and the seasonal variations in the orientation of the geomagnetic dipole axis with respect to the earth-sun line.

Because the motion and behavior of the particles under study in this paper are governed by the geomagnetic field, magnetic local time is used here instead of the usual geographic local time. For the orbit of Injun 3, magnetic local time differs by as much as  $\pm 2.3$  hours from the corresponding geographic local time.

## THE RESULTS

The magnetic local time and invariant latitude coordinates were calculated at points, eight seconds apart along the orbit of the satellite through the regions where the Electron Multiplier responded to large particle fluxes. Figure 5 shows a polar plot of these responses. Two major effects are noted. First there is an almost complete absence of responses on the day side and second, the responses on the night side occur only between  $58^\circ$  and  $76^\circ$  invariant latitude. In order to determine whether these are genuine effects or are merely due to non-uniform data sampling, we now investigate the sample density of Injun 3 data over the entire magnetic local time invariant latitude space (henceforth called the MLT-INV space).

For all useable Injun 3 data for which  $L \geq 2.0$ , the MLT and INV coordinates were calculated (16 seconds apart) along the orbit of the satellite. These coordinates were sorted into "boxes" of 1 hour intervals in MLT and  $1^\circ$  intervals in INV. All duplications of a given revolution number were eliminated from each box so that the final number in each box represented the total number of times the satellite produced good data while crossing each element in MLT-INV space. This number is therefore the number of



opportunities to observe an Electron Multiplier response in that box.

The same sort in MLT-INV space was performed on both the Electron Multiplier responses due to light and due to valid particle events. With these three sorts completed, the number in each box of the sort of the Electron Multiplier responses to sunlight was subtracted from the number in the equivalent box of the total sample density. This is necessary because once the Electron Multiplier responds to sunlight, it no longer has an opportunity to respond to a particle event in that region (although as was mentioned before only two cases were observed where a particle event might have occurred simultaneously with a light response). With the distributions in MLT-INV space for the valid particle responses and the total sample density corrected for light responses, we now investigate each effect noted in Figure 5 separately.

In order to investigate the diurnal effect we will assume for the present that the latitude effect observed in Figure 5 is genuine. Therefore, we restrict the sample density in MLT to only those boxes which lie between  $58^\circ$  and  $76^\circ$  invariant latitude.

The results of this investigation are given in Figure 6. The frequency of occurrence for  $j (E_e \geq 10 \text{ keV}) \geq 2.5 \times 10^7$

electrons  $(\text{cm}^2 \text{ sec ster})^{-1}$  is obtained by dividing the number of events occurring within a one hour local time interval by the number of independent samples taken in that interval. It is observed that the diurnal effect noted previously is valid and represents one of the most striking diurnal variations observed in geomagnetically trapped particles to date.

With this diurnal effect established we select only the region of MLT-INV space where  $17.0 \text{ hours} \leq \text{MLT} \leq 7.0 \text{ hours}$  as the appropriate body of data for investigating the latitude effect. The results of this investigation are presented in Figure 7, where again the frequency of occurrence is obtained by dividing the number of events occurring within a one degree invariant latitude interval by the number of independent samples taken in that interval. It is observed that the latitude effect noted previously is valid and that it has a rather sharp lower boundary at  $A \simeq 60^\circ$  ( $L \simeq 4.0$ ). This latitude profile is very similar to the profiles given for auroral frequency by Vestine [Ratcliffe, 1960], by Davis [1962], and by O'Brien and Taylor [1964]. Further, Meeks [1954] reported that observations made over a period of a year in 1948-1949 at Portage la Prairie and Baker Lake (geomagnetic latitude  $59^\circ \text{ N}$  and  $75^\circ \text{ N}$ ) established that there are two latitude peaks of

occurrence of aurora in the night, one being at  $65^{\circ}$  N and the other at  $68^{\circ}$  N. Davis [1962] using five all-sky cameras at various stations in Alaska found a "pronounced minimum" at  $66^{\circ}$ - $67^{\circ}$  N geomagnetic latitude in the frequency of occurrence of overhead auroras for all data from these stations from September 1957 to April 1958. On breaking the data down into various groups he found that the effect was much less prominent and finally attributed "the apparent minimum to non uniformity of the observations". If, however, the "pronounced minimum" is real, it is in agreement with the results of Meek [1954].

A similar combination of effects is evident in the latitude profile of the frequency of occurrence of the Injun 3 intense electron precipitation events, although the resolution into two peaks is of only marginal statistical significance. (The error bar in Figure 7 represents the 67% probability brackets assuming that the number of occurrences in each interval is a Poissonian variable.) It is noted also that the frequency of occurrence for aurora as a function of local time passes through a main maximum usually an hour or so in advance of local midnight [Ratcliffe, 1960], and this again is similar to that observed for the Injun 3 intense electron precipitation events in Figure 6.

Since there seems to be a strong similarity between the behavior of auroral light emission and these intense electron precipitation events, we now investigate the correlation between these electron events and geomagnetic activity. To do this we use the daily  $K_p$  sum index associated with each independent sample in MLT-INV space (with the restriction that  $17.0 \text{ hours} \leq \text{MLT} < 7.0 \text{ hours}$  and  $58^\circ \leq \lambda \leq 76^\circ$ ) as the body of data for this study. The results are presented in Figure 8 where the frequency of occurrence of  $j$  ( $E_e \geq 10 \text{ keV}$ )  $\geq 2.5 \times 10^7$  electrons ( $\text{cm}^2 \text{ sec ster}$ ) $^{-1}$  per  $K_p$  sum interval is obtained by dividing the number of events associated with a given daily  $K_p$  sum in all appropriate MLT-INV boxes by the corresponding number from the sample density tables. It is observed from Figure 8 that there is a strong tendency for intense dumping events to occur more commonly as the  $K_p$  sum value increases.

The validity of each of these effects (the diurnal, the latitude, and the positive correlation with geomagnetic activity) is independent of the absolute calibration of the Electron Multiplier and depends only on the fact that the Electron Multiplier does respond only to a particle flux exceeding some given intensity.

## SPECTRAL CHANGES

As a final point in this study, a remarkable spectral change is usually observed when the intense low energy electron fluxes are present. This change is associated with the trapping boundary for 40 keV electrons. At latitudes less than the latitude of the trapping boundary the electron energy spectrum is usually fairly "flat" between 10 keV and 40 keV. On the high latitude side of the trapping boundary, the spectral slope between 10 keV and 40 keV becomes extremely steep indicating the presence of a very soft electron spectrum.

This spectral change is observed on both northbound and southbound passes and is therefore a spatial and not a temporal effect. Figures 9 and 10 give an example of each type of pass. Using the observation reported by O'Brien [1964] that the angular distribution of the directional electron flux tends to approach isotropy over the upper hemisphere at the altitude of the satellite during intense precipitation events involving electrons with  $E_e \geq 40$  keV (in Appendix II, the validity of applying this observation to the present study is demonstrated), we can calculate spectral parameters using the Electron Multiplier ( $\alpha \sim 50^\circ$ ) and SpL ( $\alpha \sim 90^\circ$ ). A set of spectral parameters is calculated for sample points inside and outside

the trapping boundary in both Figures 9 and 10. The parameter  $E_0$  is e-folding energy in a differential exponential spectral form ( $dN/dE = N_0 e^{-E/E_0}$ ) and the parameter  $\gamma$  is the exponent in a differential power-law spectral form ( $dN/dE = KE^{-\gamma}$ ). In each figure, these parameters demonstrate the remarkable softening of the electron energy spectrum between 10 keV and 40 keV in crossing the 40 keV electron trapping boundary. A more complete study of these spectral changes is now being performed and will be discussed in greater detail in a later paper. In the present paper we only indicate the existence of these unusual spectral changes and leave the details to a later paper.

## CONCLUSIONS

In the present paper we have observed and discussed the following effects derived from data of the Electron Multiplier detector on satellite Injun 3:

1. The observation of the existence of intense fluxes up to  $10^9$  electrons  $(\text{cm}^2 \text{ sec ster})^{-1}$  (see Figure 12) of 10 keV electrons associated with the trapping boundary for 40 keV electrons.
2. A large diurnal variation in the frequency of occurrence for  $j (E_e \geq 10 \text{ keV}) \geq 2.5 \times 10^7$  electrons  $(\text{cm}^2 \text{ sec ster})^{-1}$ . These events occur only during local night between 1700 hours and 0700 hours (Figure 6).
3. A large latitude variation for the frequency of occurrence of  $j (E_e \geq 10 \text{ keV}) \geq 2.5 \times 10^7$  electrons  $(\text{cm}^2 \text{ sec ster})^{-1}$ . These events occur only between  $58^\circ$  and  $76^\circ$  invariant latitude and seem to be strikingly similar in behavior to the frequency of occurrence of auroral light emission as a function of invariant latitude (Figure 7).
4. A strong positive correlation between the frequency of occurrence of these intense low energy electron precipitation events and geomagnetic activity (Figure 8).

5. The existence of a large change in the slope of the electron energy spectrum between 10 keV and 40 keV associated with the trapping boundary for 40 keV electrons during events of this nature. The change is from a fairly hard spectrum inside the boundary to a very soft spectrum just outside the boundary.

We will now see how these results fit in with the previous observations which have been published on low energy electrons in the outer Van Allen radiation belt.



## COMMENTS

The present study provides a fuller diurnal and latitude study of intense low energy electron precipitation events than any previously published study. There are a number of individual observations of these intense precipitation events with low altitude satellites which we will review.

The single intense event reported by O'Brien and Laughlin [1962] occurred at approximately 1900 hours local time between invariant latitudes of  $70^\circ$  and  $72^\circ$  on September 25, 1961. The  $K_p$  daily sum for that day was 33 $\alpha$ , the highest during the entire month. This event therefore is in agreement with the conclusions of the present study.

Sharp et al. [1964a] reported the existence of large energy fluxes for five passes through the northern auroral zone on March 1-3, 1962. Their polar-orbiting satellite was fixed for this short period to local times of approximately 2000 hours since telemetry apparently was taken only over Alaska. These results then agree with those of the present paper. Sharp et al. [1964b] using a similar polar orbiting satellite observed precipitating electrons of energy greater than 80 eV at approximately 0100 and 1300 hours local time every 90 minutes throughout the period from October 31 to November 4,

1963. They observed that the total precipitated energy was considerably larger (by approximately a factor of five) on the night side than on the day side. They noted that the total precipitated energy correlated generally with the  $K_p$  index and with the K index of a local station near the satellite at the time the data were taken. Finally they reported that a preliminary analysis showed the spectral shape to be harder on the day side than on the night side in the northern auroral zone. All of these findings appear to be in agreement with the results of this paper.

Results of a somewhat different nature have been reported by Krasovskii et al. [1962]. Of the four passes on which they report large fluxes of 10 keV electrons precipitating into the atmosphere, three of the passes have local times which agree with results of the present study but all four passes occur at much lower latitudes. In fact a majority of their responses occur inside the classical inner zone,  $L < 2.0$  ( $A < 45^\circ$ ). It appears that Krasovskii et al. are dealing with a different phenomenon than that of the present paper. Therefore the results of the present study appear to be in general agreement with more limited observations published previously in the literature at low satellite altitudes.

We suggest that these intense low energy electron fluxes found near the trapping boundary for 40 keV electrons at low satellite altitudes are related to the intense fluxes of low energy electrons found by Gringauz et al. [1962] and by Freeman [1964] at great distances on the night side of the earth.

TABLE I

Pt. No.	Revolution	L	B	$\alpha$	Validity Check	$E_0$	$J$ ( $> 10$ keV)	E.M. Response c/s
1	90	1.74	.110	89°	+ 27%	97	$1.85 \times 10^7$	$1.0 \times 10^{-1}$
2	90	1.61	.102	69°	+ 35%	92	$3.08 \times 10^7$	$1.94 \times 10^{-1}$
3	104	1.69	.170	82°	+ 9%	109	$6.50 \times 10^6$	$3.47 \times 10^{-2}$
4	105	1.53	.161	72°	+ 8%	94	$1.08 \times 10^7$	$6.33 \times 10^{-2}$
5	105	1.65	.182	70°	+ 10%	109	$4.60 \times 10^6$	$3.27 \times 10^{-2}$
6	105	1.75	.197	72°	+ 11%	98	$3.80 \times 10^6$	$1.92 \times 10^{-2}$
7	115	1.64	.110	58°	+ 38%	97	$1.65 \times 10^7$	$1.08 \times 10^{-1}$
8	136	1.79	.118	74°	+ 1.9%	100	$1.13 \times 10^7$	$6.67 \times 10^{-2}$
9	141	1.65	.117	70°	+ 13%	112	$1.60 \times 10^7$	$1.03 \times 10^{-1}$
10	148	1.81	.122	70°	+ 3.5%	99	$9.3 \times 10^6$	$5.56 \times 10^{-2}$
11	148	1.74	.122	85°	+ 1%	100	$1.37 \times 10^7$	$8.33 \times 10^{-2}$
12	148	1.73	.122	71°	+ 5%	105	$1.17 \times 10^7$	$6.67 \times 10^{-2}$

## APPENDIX I

Magnetic Local Time

As used here Magnetic Local Time (MLT) is defined as the angle between the magnetic meridians which pass through the observation point and then through the sun. This definition corresponds to the definition of geomagnetic time given by Chamberlain [1961]. Geomagnetic time has been used to organize auroral data [Vegard, 1912] and is used here to organize high latitude data from a satellite.

To calculate MLT we define the following quantities. Let  $\vec{P}$  be a unit vector directed from the center of the earth to the observation point. The observation point has local time coordinate LT and latitude coordinate  $\lambda$ . Let  $\vec{S}$  be a unit vector in the antisolar direction, and let  $\vec{m}$  be a unit vector along the axis of symmetry of the geomagnetic field. Magnetic local time is the angle of intersection between the  $(\vec{P}, \vec{S})$  plane and the  $(\vec{P}, \vec{m})$  plane. The relationship between these vectors and the rotational axis of the earth ( $\vec{R}$ ) is shown in Figure 11. The angle  $\delta$  is the solar declination. Local magnetic time increases in the right hand sense relative to  $\vec{m}$  and is calculated using:

$$\text{MLT} = \frac{12}{\pi} \cos^{-1} \frac{(\vec{S} \times \vec{m}) \cdot (\vec{P} \times \vec{m})}{|\vec{S} \cdot \vec{m}| |\vec{P} \cdot \vec{m}|}$$

The branch of  $\cos^{-1}$  is determined from the sign of  $\vec{S} \times (\vec{P} \times \vec{m})$ : MLT is between 0-12 hours and 12-24 hours when  $\vec{S} \times (\vec{P} \times \vec{m})$  is positive or negative, respectively.

The axis of symmetry ( $\vec{m}$ ) of the geomagnetic field has been taken as the axis of the centered dipole approximation for the geomagnetic field. The axis points used are those quoted by Chapman and Bartels [1940], and are at  $\lambda_m = 78.5^\circ$  N latitude,  $69^\circ$  W longitude, and at  $78.5^\circ$  S latitude,  $111^\circ$  E longitude. ( $\theta_p$  in Figure 11 is equal to  $\pi/2 - \lambda_m$ .) At the highest latitude reached by Injun III ( $70.3^\circ$ ) the maximum difference between MLT and LT is +2.3 hours. At higher latitudes the effects of the displacement of the dipole from the earth's center become increasingly important and magnetic local time should be calculated using the eccentric dipole approximation.

The definition of magnetic local time incorporates two symmetries which make it a useful coordinate for organizing measurements in the earth's magnetosphere. The interaction of the solar wind with the geomagnetic field is invariant under the following operations: First, if the solar wind velocity is

along  $\vec{S}$  and the effect of the interplanetary magnetic field can be neglected then the system is invariant under a rotation about  $\vec{S}$ . Second, to the first order of approximation for the geomagnetic field the system is invariant under a rotation of the earth about  $\vec{m}$ . In successive observations having the same magnetic solar declination ( $\delta_m = \sin^{-1} \vec{S} \cdot \vec{m}$ ) points having the same spatial relationship relative to  $\vec{S}$  and  $\vec{m}$  are equivalent for observing processes having time scales short compared to the rotational period of the earth. These comments show the utility of using  $\vec{S}$  and  $\vec{m}$  to define a coordinate system for analyzing magnetospheric data. A convenient set of coordinates is for example: MLT, invariant latitude  $\Lambda$ ,  $B$ , and magnetic solar declination  $\delta_m$ .

## APPENDIX II

In the text of this paper we have made the assumption that the Electron Multiplier is measuring fluxes of 10 keV electrons and not similar fluxes of 50 keV protons. This assumption cannot be proved but plausibility arguments can be given which apply to a majority, but not all, of the events observed.

On Injun 3, as we previously mentioned, detector 1 is an open end, thin window, 213-type Geiger tube. It measures the flux of electrons with energy greater than 40 keV or the flux of protons with energy greater than 500 keV, traveling perpendicular to the geomagnetic field line at the position of the satellite ( $\alpha = 90^\circ \pm 13^\circ$ ). Detector 5 is similar to detector 1 but measures fluxes which are traveling down the field line ( $\alpha = 0^\circ \pm 43^\circ$ ). The SpL detector measures only electrons with pitch angles of  $90^\circ \pm 6^\circ$  which have energies between 40 keV and 55 keV. The responses of these detectors are presented in Figure 12 for two of the events used in the present paper.

O'Brien [1964] found that during intense precipitation events involving electrons with  $E_e \geq 40$  keV, the angular distribution of the directional electron flux tends to approach isotropy over the upper hemisphere at the altitude of the



satellite. In Figure 12, since  $j_{\alpha=90^\circ} (E_e \geq 40 \text{ keV or } E_p \geq 500 \text{ keV}) = j_{\alpha=0^\circ} (E_e \geq 40 \text{ keV or } E_p \geq 500 \text{ keV})$  we observe the effect reported by O'Brien [1964]. This means that we can compare the flux measured by the Electron Multiplier ( $\alpha = 50^\circ \pm 10^\circ$ ) with that measured by the  $\alpha = 90^\circ$  detectors.

We also observed that  $j_{\alpha=90^\circ} (E_e \geq 40 \text{ keV or } E_p \geq 500 \text{ keV}) = j_{\alpha=90^\circ} (40 \text{ keV} \leq E_e \leq 55 \text{ keV})$ . This means that the total flux of protons with  $E_p \geq 500 \text{ keV}$  is negligibly small in comparison to the total flux of electrons with  $E_e \geq 40 \text{ keV}$ . The electron spectrum can be measured above 40 keV and in these two events is very steeply rising toward lower energies.

It is argued that the Electron Multiplier must be responding to electrons with  $E_e \geq 10 \text{ keV}$  since any other response would entail a drastic change in the electron energy spectrum between 10 keV and 40 keV and would require a proton spectrum which has an unreasonably large slope between 50 keV and 500 keV.

As a further argument, it is noted that Evans et al. [1963] found that fluxes of protons precipitated into the auroral zones varied in a smooth manner (readings taken 0.2 seconds apart) in contrast with the large intensity changes

in the electron fluxes measured simultaneously. We observe from Figure 12 that there are large intensity variations in times of the order of a fraction of a second in the flux measured by the Electron Multiplier, again indicating that it is probably responding to the electrons and not to protons.

For the 84 individual events used in this study, arguments of this kind can be applied to 72 (~ 86%) of them. Four more had extremely soft spectrums and no determination could be made. The remaining eight events gave inconclusive arguments of this nature but did indicate the presence of a large fraction of electrons in the total flux measured by detector 1.

On the basis of these arguments we conclude that the Electron Multiplier is responding to electrons with  $E_e \geq 10$  keV for the events presented in the present paper.

## ACKNOWLEDGEMENTS

We would like to express our thanks to Professor James A. Van Allen for his suggestions and advice concerning the in flight calibration procedure and the study itself.

Our thanks are extended to Mr. Donald E. Stilwell for the construction and preflight calibration of the Electron Multiplier and to Mr. Curt Zimansky for assisting in the reduction of the data.

This work was supported in part by the Office of Naval Research under contract Nonr 1509(06) and by the National Aeronautics and Space Administration under grant NsG-233-62.

## REFERENCES

- Armstrong, T., The morphology of the outer zone electron distribution of low altitudes from January through July and September, 1963 from Injun III, SUI Research Report 64-40, 88 pp., 1964.
- Bruining, H., Physics and Applications of Secondary Electron Emission, McGraw-Hill, New York, 1954.
- Chamberlain, J. W., Physics of the Aurora and Airglow, Academic Press, New York, 1961.
- Chapman, S., and S. Akasofu, The Aurora, in Research in Geophysics, edited by H. Odishaw, Chapter 15, M.I.T. Press, 1964.
- Chapman, S., and J. Bartels, Geomagnetism, Clarendon Press, Oxford, 1940.
- Davis, T. N., The morphology of the auroral displays of 1957-1958. 1. Statistical analyses of Alaska data, J. Geophys. Res., 67, 59-74, 1962.
- Evans, J. E., R. G. Johnson, R. D. Sharp, and J. B. Reagan, Precipitated proton fluxes at 300 km altitude over the auroral zones, Paper GA24 presented at the Annual AGU Meeting, Washington, 1963.
- Frank, L. A., Efficiency of a Geiger-Mueller tube for non-penetrating electrons, J. Franklin Inst., 273, 91-106, 1962.
- Frank, L. A., J. A. Van Allen, and J. D. Craven, Large diurnal variations of geomagnetically trapped and of precipitated electrons observed at low altitudes, J. Geophys. Res., 69, 3155-3167, 1964.

- Freeman, J. W., The morphology of the electron distribution in the outer radiation zone and near the magnetospheric boundary as observed by Explorer 12, J. Geophys. Res., 69, 1691-1724, 1964.
- Gringauz, K. I., V. G. Kurt, V. I. Moroz, and I. S. Shklovskii, Ionized gas and fast electrons in the vicinity of the earth and in interplanetary space, Planet. Space Sci., 9, 21-25, 1962.
- Krasovskii, V. I., I. S. Shklovskii, Yu. I. Gal'perin, E. M. Svetlitskii, Yu. M. Kushnir, and G. A. Bordovskii, The detection of electrons with energies of approximately 10 keV in the upper atmosphere, Planet. Space Sci., 9, 27-40, 1962.
- Laughlin, C. D., A satellite borne magnetic electron spectrometer, SUI Research Report 60-14, August, 1960, 79 pp.
- McDiarmid, I. B., and E. E. Budzinski, Angular distributions and energy spectra of electrons associated with auroral events, Can. J. Phys., 42, 2048-2062, 1964a.
- McDiarmid, I. B., and J. R. Burrows, Diurnal intensity variation in the outer radiation zone at 1000 km, Can. J. Phys., 42, 1135-1148, 1964b.
- McDiarmid, I. B., D. C. Rose, and E. Budzinski, Direct measurement of charged particles associated with auroral zone radio absorption, Can. J. Phys., 39, 1888, 1961.
- McIlwain, C. E., Direct measurement of protons and electrons in visible aurorae, Space Research, North Holland, 715, 1960.

- McIlwain, C. E., Coordinates for mapping the distribution of magnetically trapped particles, J. Geophys. Res., 66, 3681-3691, 1961.
- Meek, J. H., Correlation of magnetic, auroral, and ionospheric variations at Saskatoon, Part 2., J. Geophys. Res., 59, 87, 1954.
- Meredith, L. H., L. R. Davis, J. P. Heppner, and O. E. Berg, Rocket auroral investigations, IGY Rocket Rept. No. 1, 169, 1958.
- O'Brien, B. J., Lifetimes of outer-zone electrons and their precipitation into the atmosphere, J. Geophys. Res., 67, 3687-3706, 1962.
- O'Brien, B. J., Review of studies of trapped radiation with satellite-borne apparatus, Space Science Reviews, 1, 415-484, 1963.
- O'Brien, B. J., High-latitude geophysical studies with satellite Injun 3. 3. Precipitation of electrons into the atmosphere, J. Geophys. Res., 69, 13-43, 1964.
- O'Brien, B. J., and C. D. Laughlin, An extremely intense electron flux at 1000 km altitude in the auroral zone, J. Geophys. Res., 67, 2667-2672, 1962.
- O'Brien, B. J., C. D. Laughlin, and D. A. Gurnett, High-latitude geophysical studies with satellite Injun 3. 1. Description of the satellite, J. Geophys. Res., 69, 1-12, 1964.
- O'Brien, B. J., and H. Taylor, High-latitude geophysical studies with satellite Injun 3. 4. Auroras and their excitation, J. Geophys. Res., 69, 45-63, 1964.

- Pizzella, G., C. D. Laughlin, and B. J. O'Brien, Note on the electron energy spectrum in the inner Van Allen belt, J. Geophys. Res., 67, 3281-3288, 1962.
- Ratcliffe, J. A., Physics of the Upper Atmosphere, Academic Press, New York, 1960.
- Sharp, R. D., J. E. Evans, W. L. Imhof, R. G. Johnson, J. B. Reagan, and R. V. Smith, Satellite measurements of low-energy electrons in the northern auroral zone, J. Geophys. Res., 69, 2721-2730, 1964a.
- Sharp, R. D., J. E. Evans, R. G. Johnson, and J. B. Reagan, Measurement of total energy flux of electrons precipitating on auroral zones, presented at the Proceedings of the Fifth International Space Science Symposium, Florence, Italy, 1964b.
- Stilwell, D. E., Observations of intense, low energy electron fluxes in the outer zone during January and March, 1963, SUI Research Report 63-28, 111 pp., 1963.
- Van Allen, J. A., Direct detection of auroral radiation with rocket equipment, Proceedings of the National Academy of Sciences, 43, 57-92, 1957.
- Vegard, L., On the properties of the rays producing aurorae borealis, Phil. Mag., 23, 211-237, 1912.
- West, H. I., L. G. Mann, and S. D. Bloom, Some electron spectra in the radiation belts in the fall of 1962, Lawrence Radiation Laboratory Technical Report UCRL-7659, 38 pp., 1964.

## FIGURE CAPTIONS

- Figure 1. Four examples of the Electron Multiplier response as a function of pitch angle. In each example the Electron Multiplier response can be compared to the SpB response which is primarily due to penetrating protons and to bremsstrahlung. The large change in the SpB response in the lower right example is the result of the satellite's moving into a region of higher intensity. These examples demonstrate that the Electron Multiplier is responding to particles.
- Figure 2. Results of the inflight calibration of the Electron Multiplier. This is a plot of the in flight calibration points listed in Table I along with the response predicted on the basis of preflight calibrations.
- Figure 3. Preflight and post-launch calibration of the Electron Multiplier energy response function. The difference in the response functions is probably due to contamination of the dynode surfaces of the multiplier by the absorption of atmospheric gases prior to launch.
- Figure 4. Maximum Electron Multiplier responses to direct sunlight during the active lifetime of Injun 3. These responses demonstrated that the gain remained constant and the foil remained intact for the Electron Multiplier during the 10 month lifetime of the satellite.
- Figure 5. Polar plot for the occurrence of  $j$  ( $E_e \geq 10$  keV)  $\geq 2.5 \times 10^7$  electrons ( $\text{cm}^2 \text{ sec ster}$ ) $^{-1}$  as a function of magnetic local time and invariant latitude.



Figure 6. Frequency of occurrence for  $j$  ( $E_e \geq 10$  keV)  $\geq 2.5 \times 10^7$  electrons  $(\text{cm}^2 \text{ sec ster})^{-1}$  as a function of magnetic local time.

Figure 7. Frequency of occurrence for  $j$  ( $E_e \geq 10$  keV)  $\geq 2.5 \times 10^7$  electrons  $(\text{cm}^2 \text{ sec ster})^{-1}$  as a function of invariant latitude.

Figure 8. Frequency of occurrence for  $j$  ( $E_e \geq 10$  keV)  $\geq 2.5 \times 10^7$   $(\text{cm}^2 \text{ sec ster})^{-1}$  as a function of geomagnetic activity.

Figure 9. An example of a southbound pass demonstrating the large amount of softening of the electron energy spectrum between 10 keV and 40 keV associated with the 40 keV trapping boundary.

Figure 10. An example of a northbound pass demonstrating the large amount of softening of the electron energy spectrum between 10 keV and 40 keV associated with the 40 keV trapping boundary.

Figure 11. Coordinate system for the calculation of magnetic local time.  $\vec{R}$  is the rotational axis of the earth;  $\hat{S}$  is a unit vector in the antisolar direction;  $\hat{m}$  is a unit vector along the axis of symmetry of the geomagnetic field; and  $\hat{P}$  is a unit vector from the center of the earth to the observation point.

Figure 12. Two typical Electron Multiplier events. These events demonstrate that the probable response of the Electron Multiplier is to electrons with  $E_e \geq 10$  keV and not to protons with  $E_p \geq 50$  keV.

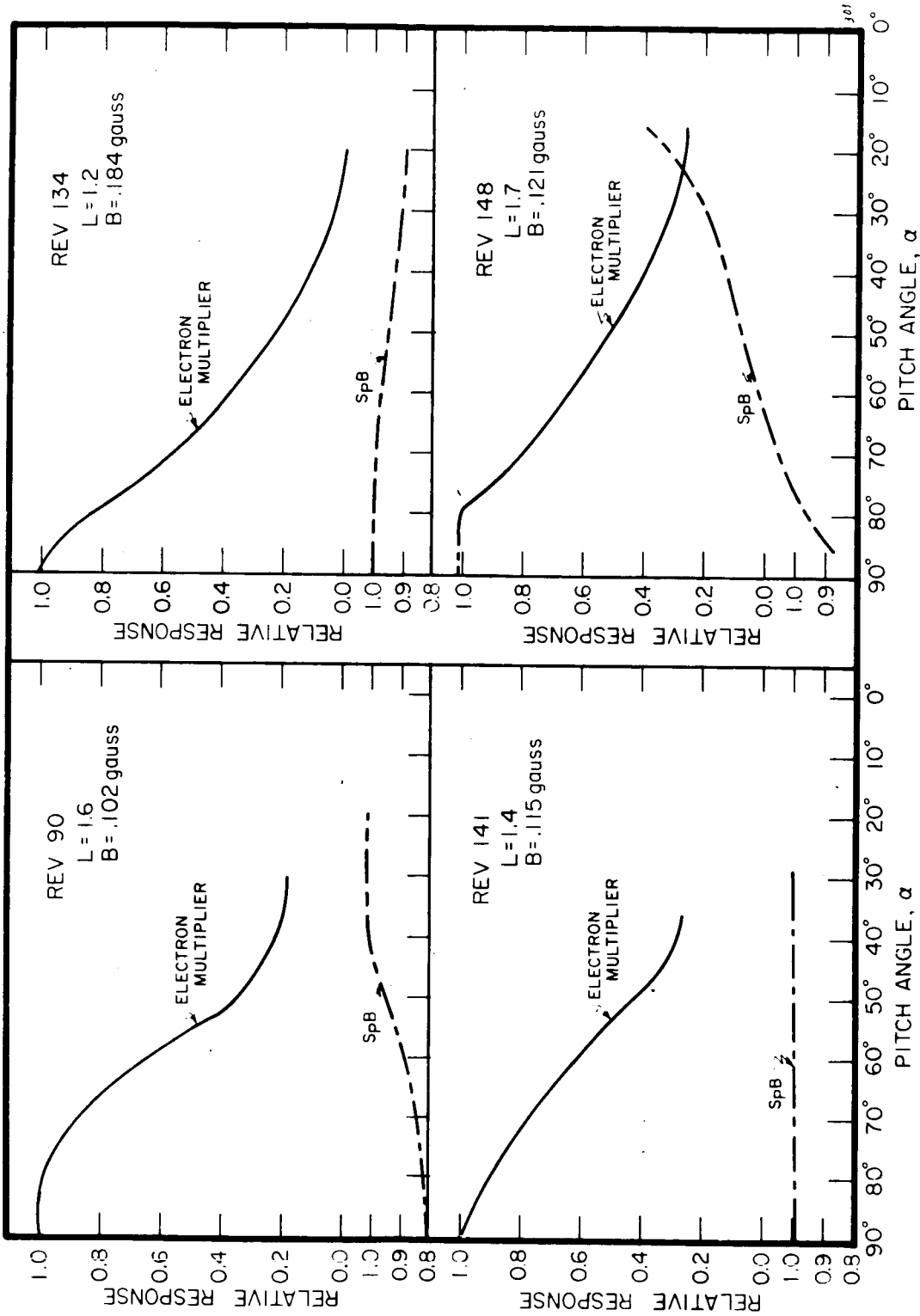


Figure 1

ELECTRON MULTIPLIER INFLIGHT  
CALIBRATIONS

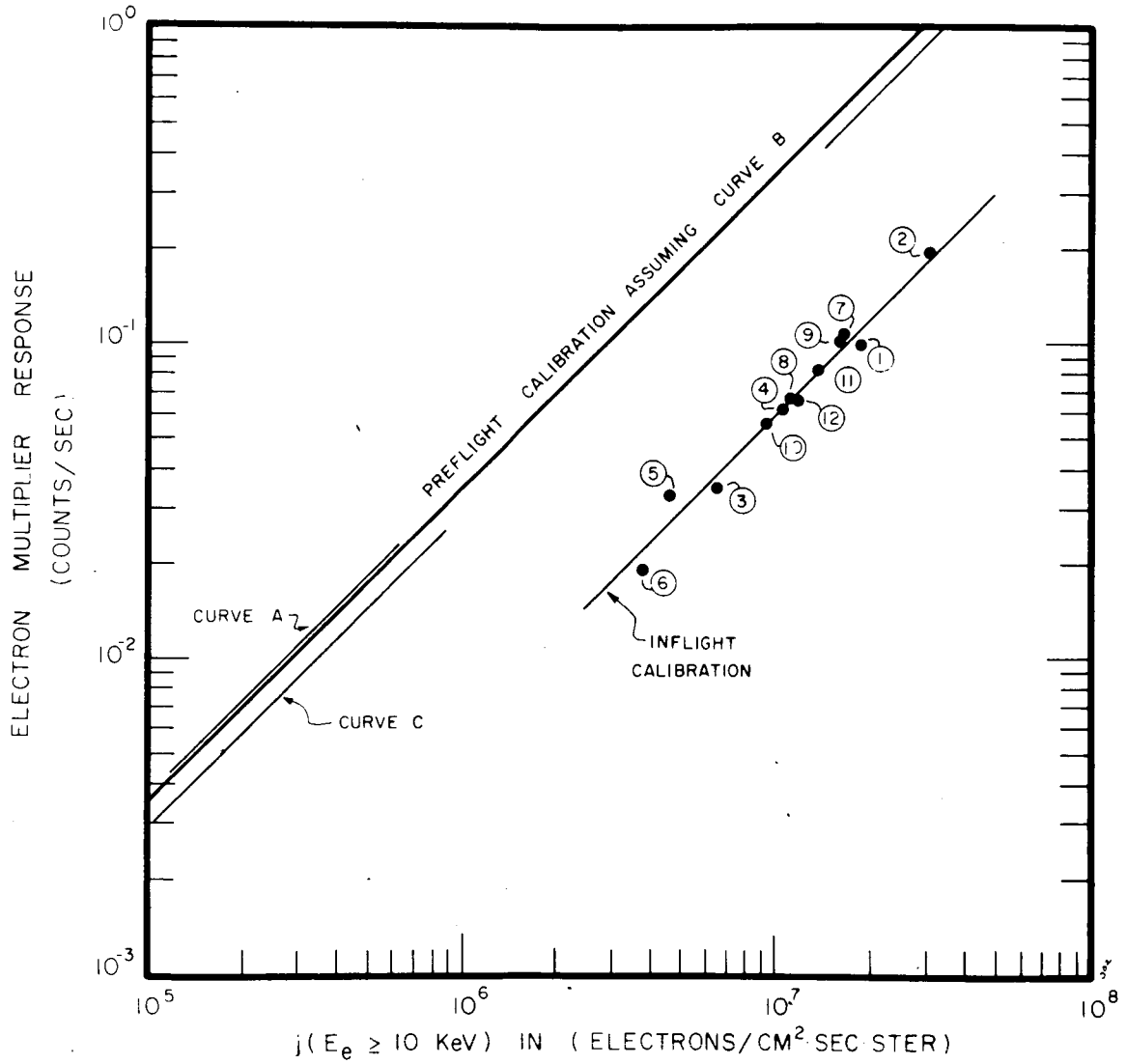


Figure 2

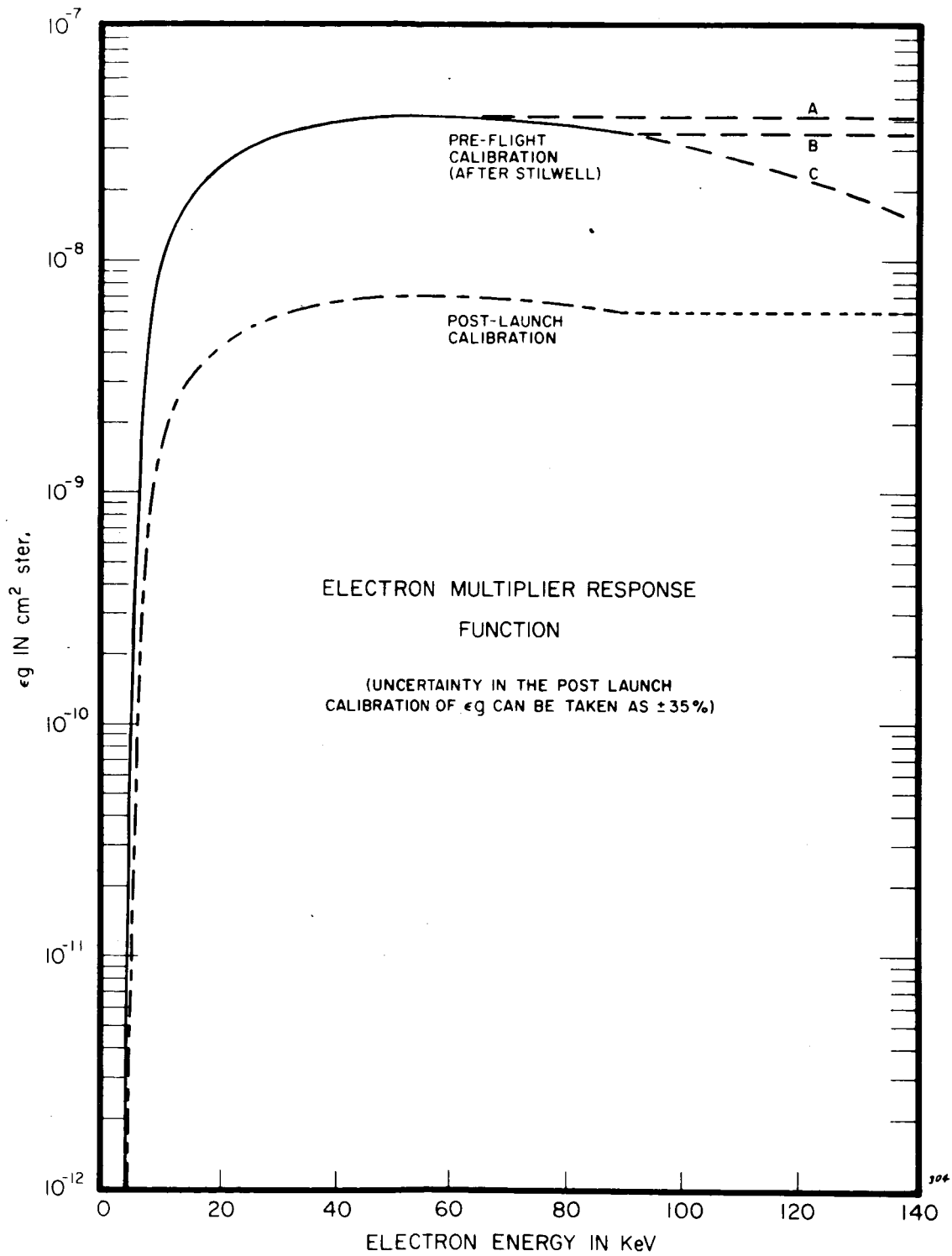


Figure 3

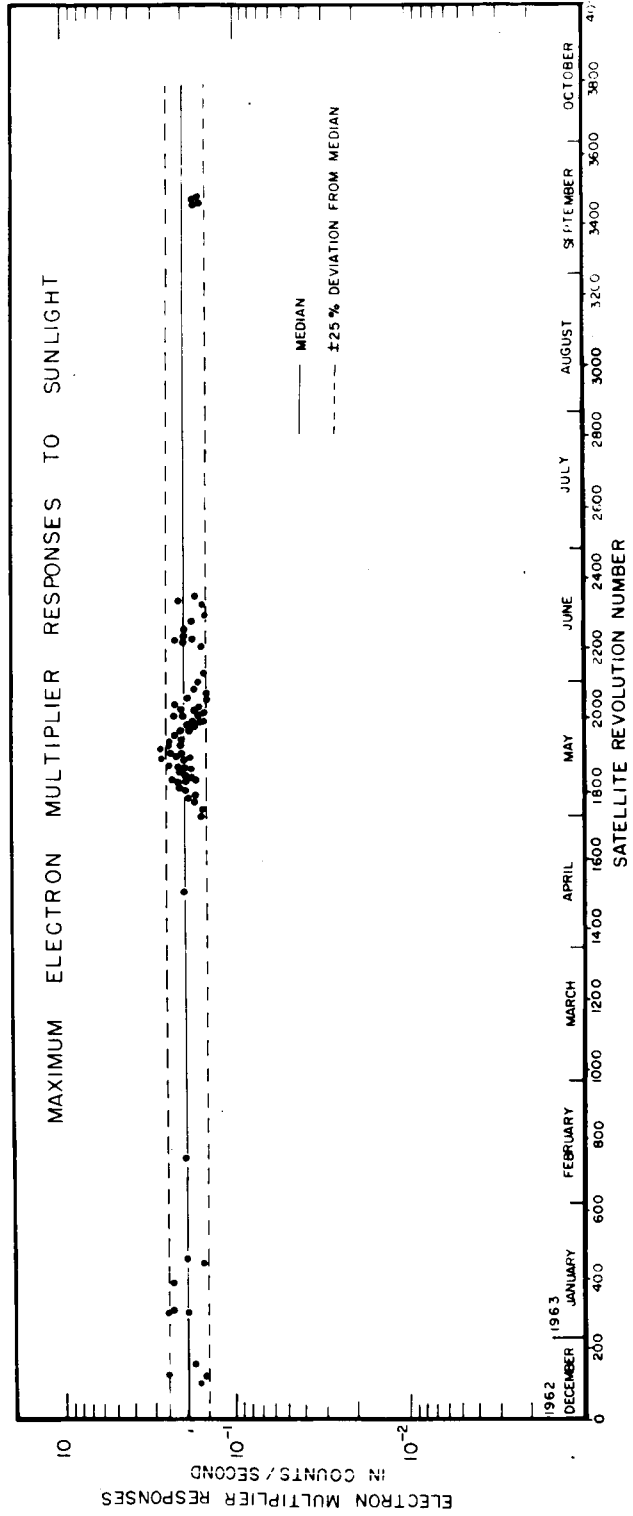


Figure 4

MAGNETIC LOCAL TIME VS. INVARIANT LATITUDE PLOT  
OF  $J(E_e \approx 10 \text{ KeV}) \approx 2.5 \times 10^7 \text{ ELECTRONS (CM}^2 \text{ SEC} \cdot \text{STER)}^{-1}$

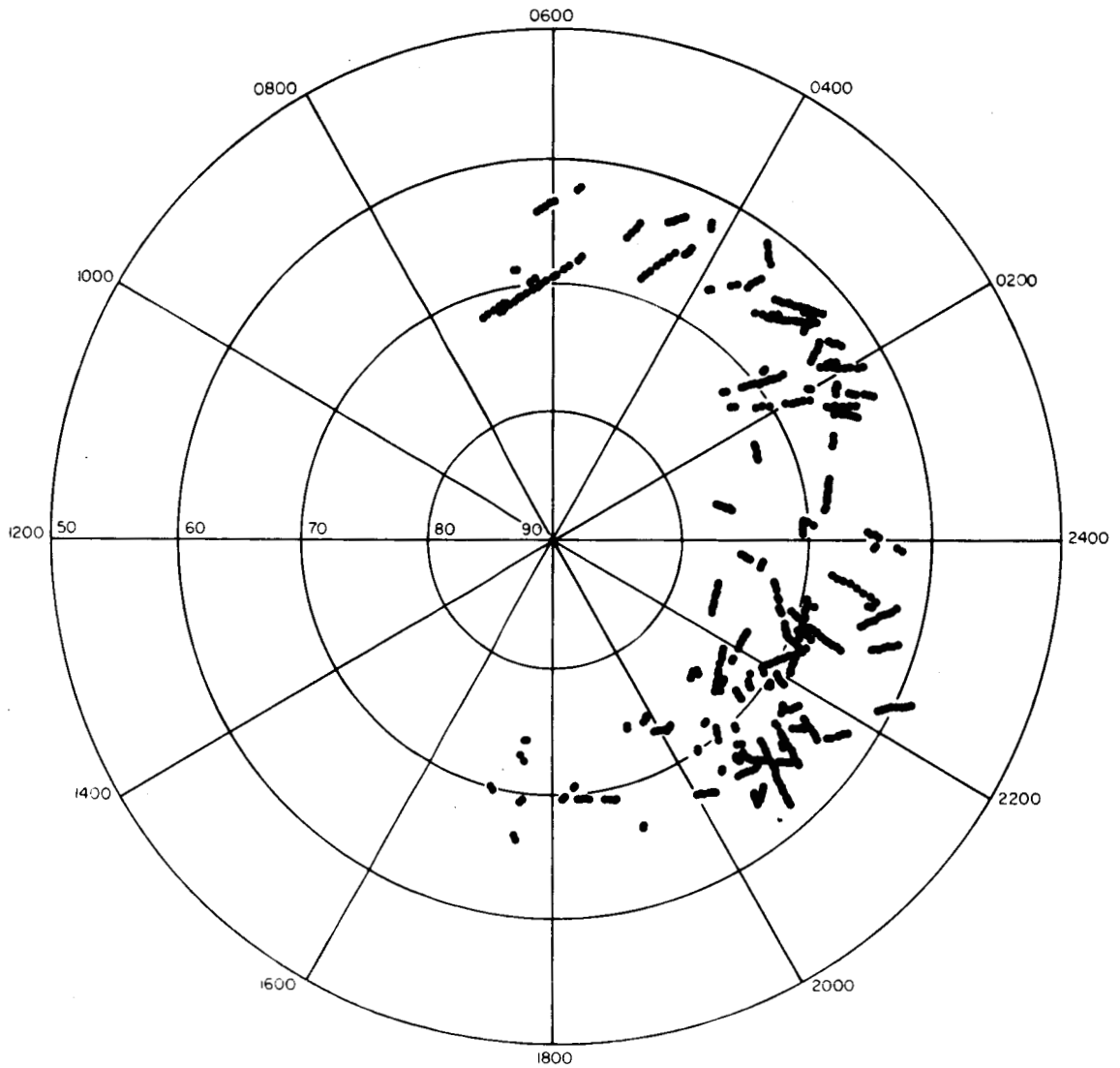


Figure 5

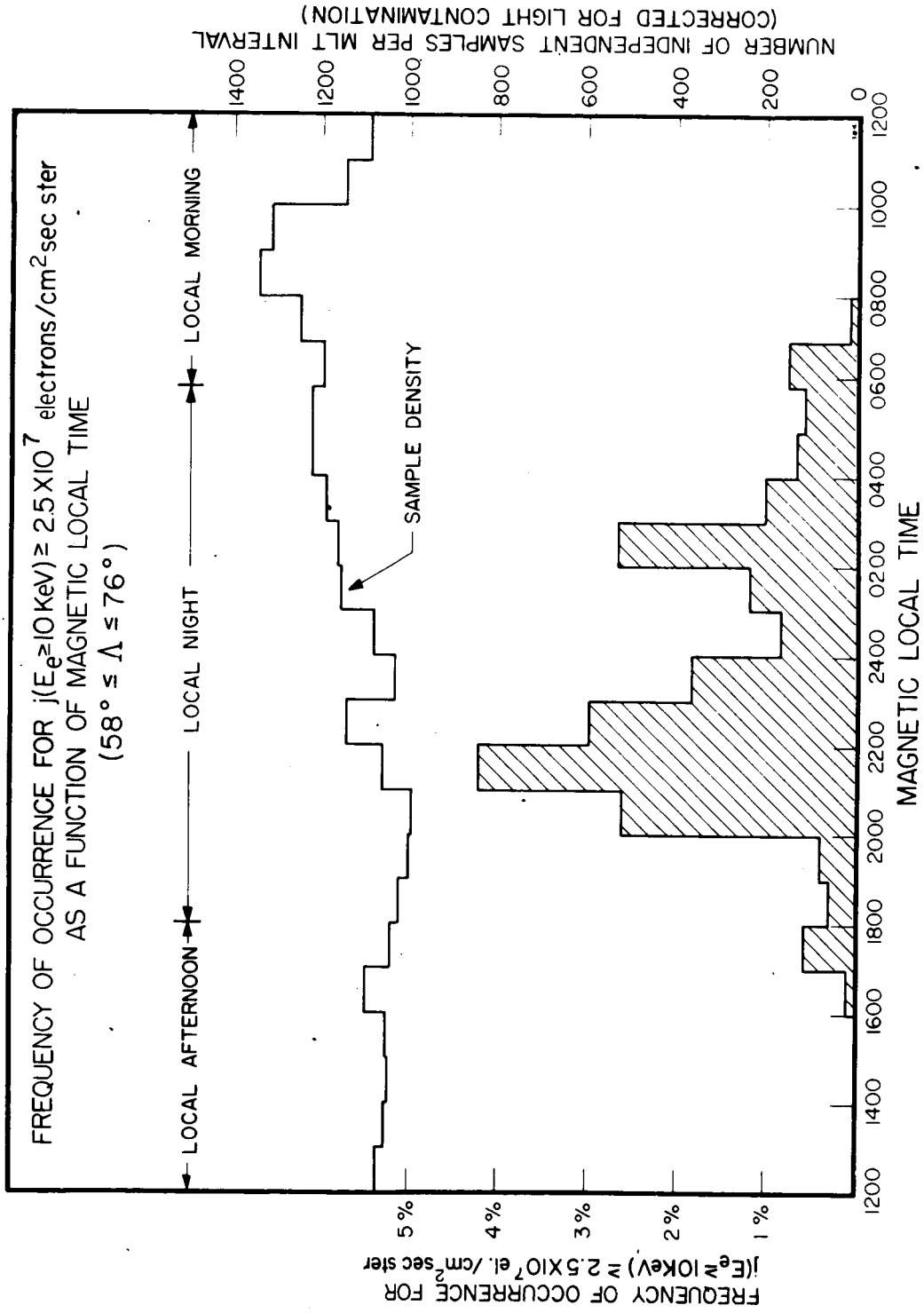


Figure 6

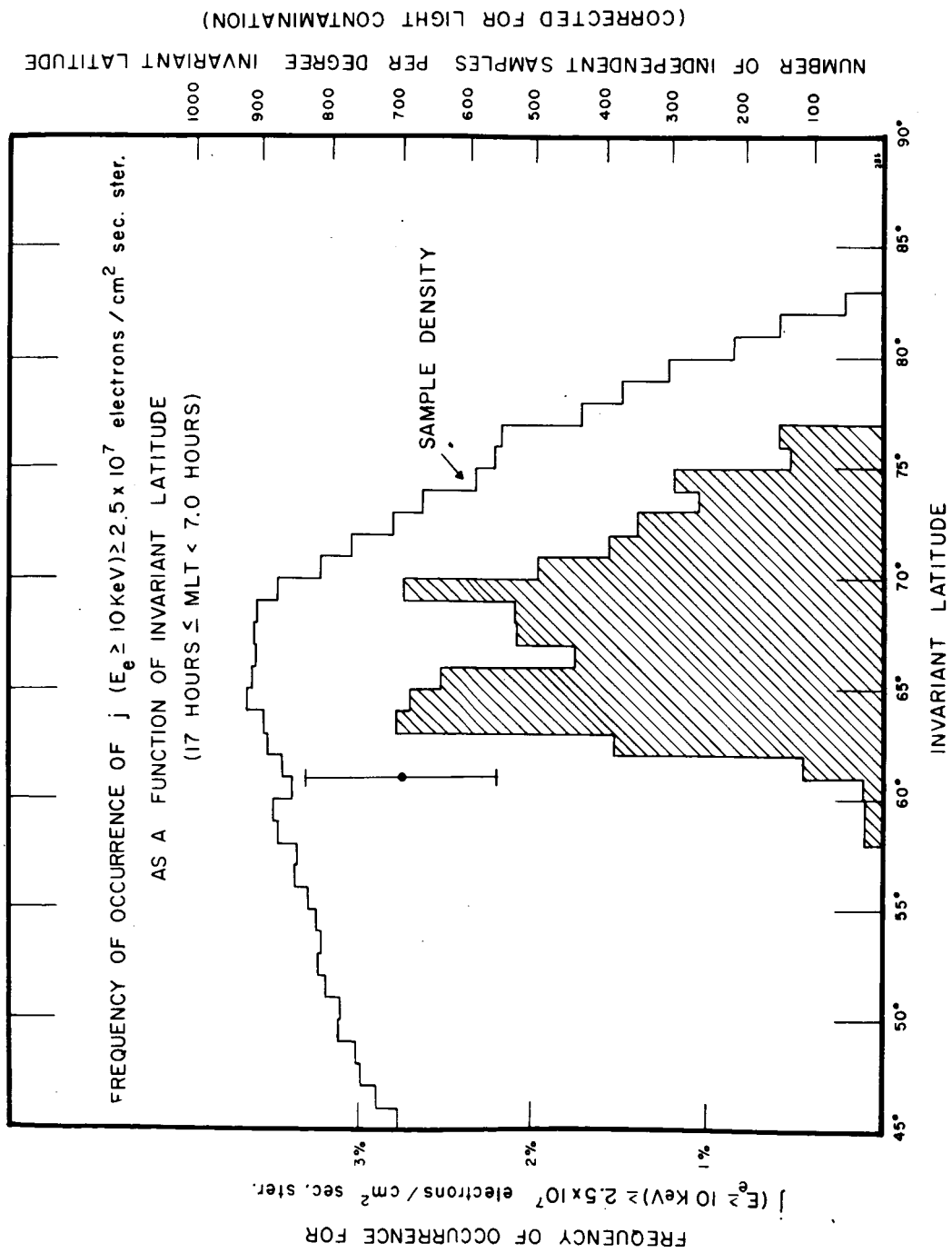


Figure 7



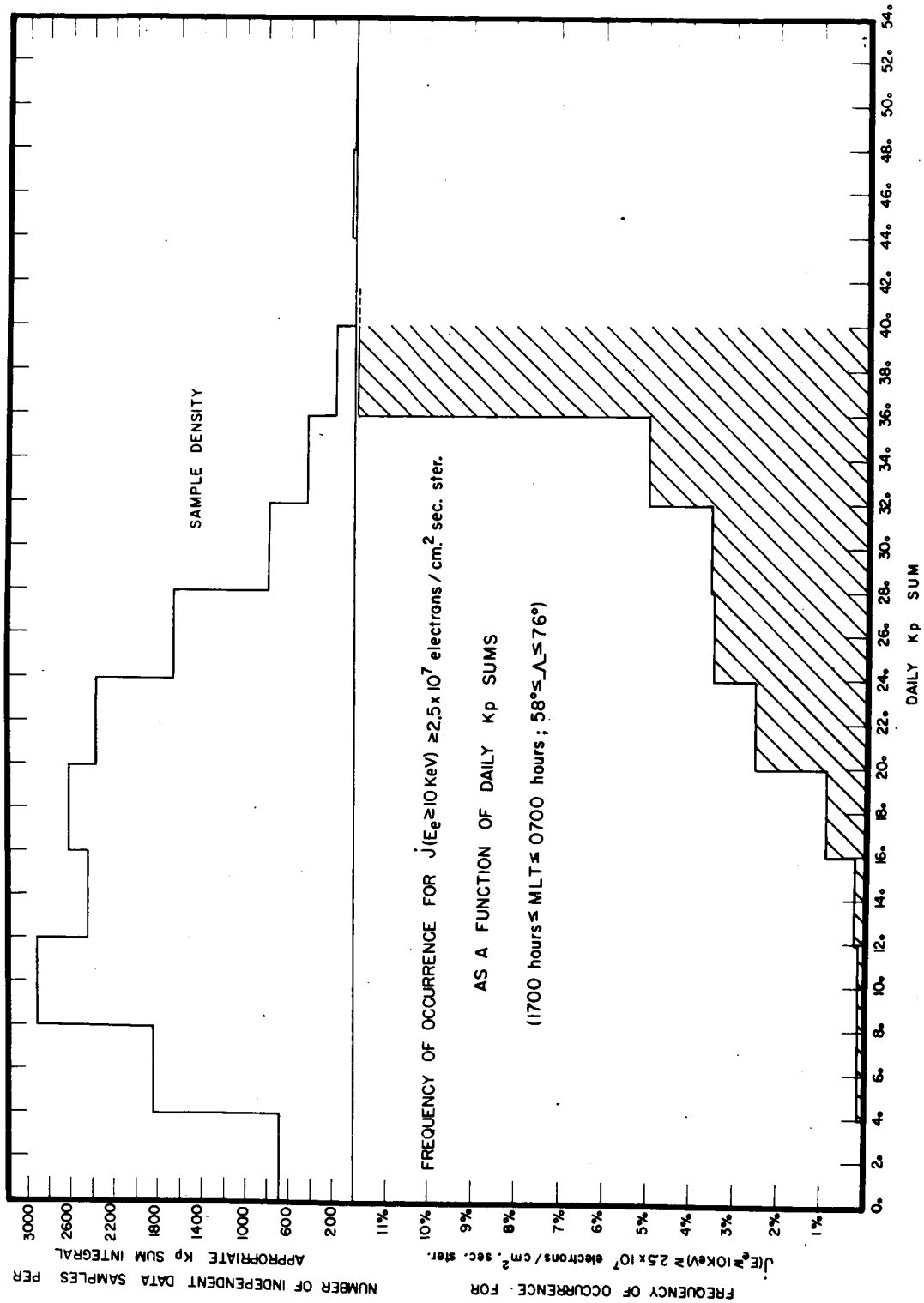


Figure 8

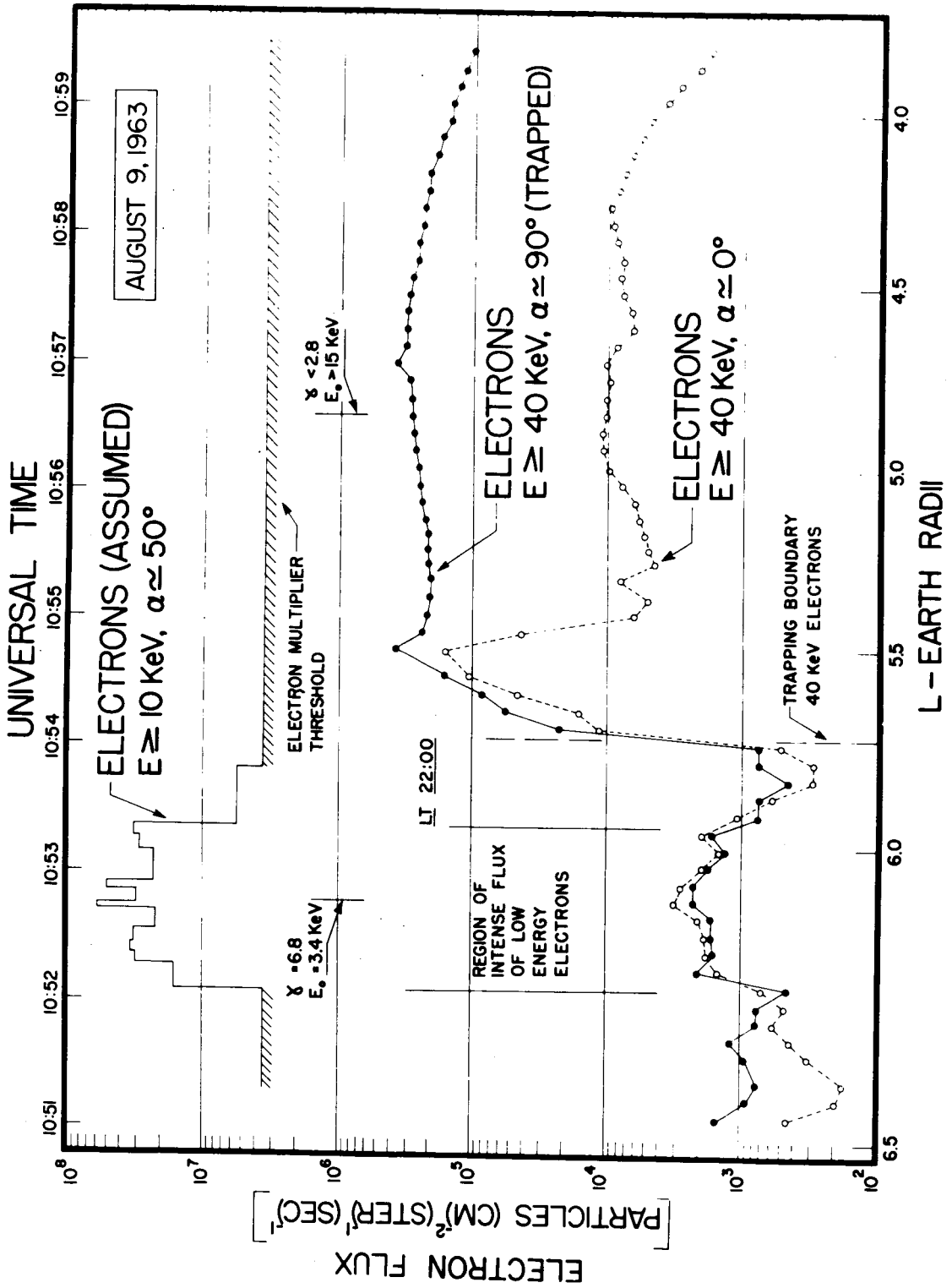


Figure 9

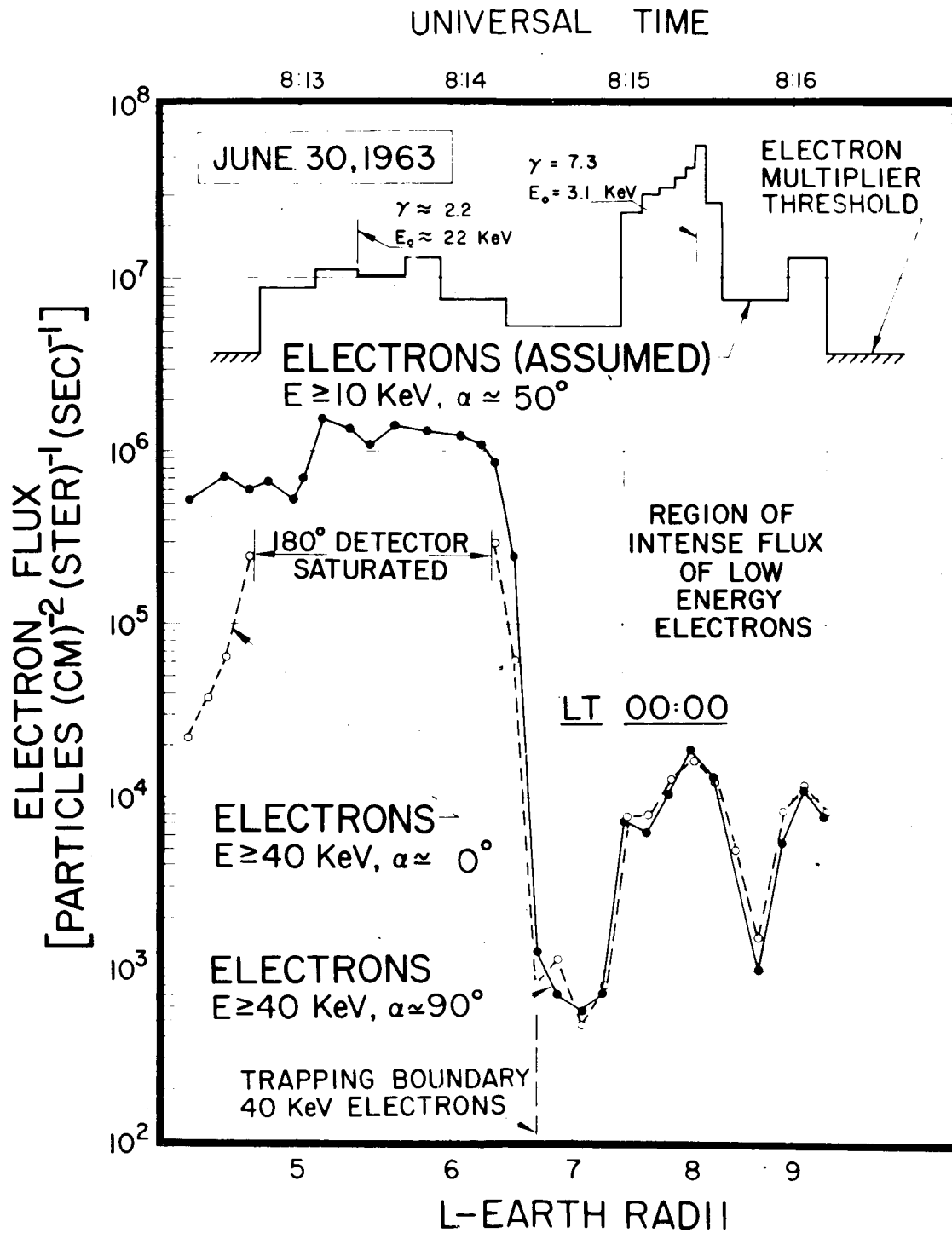


Figure 10

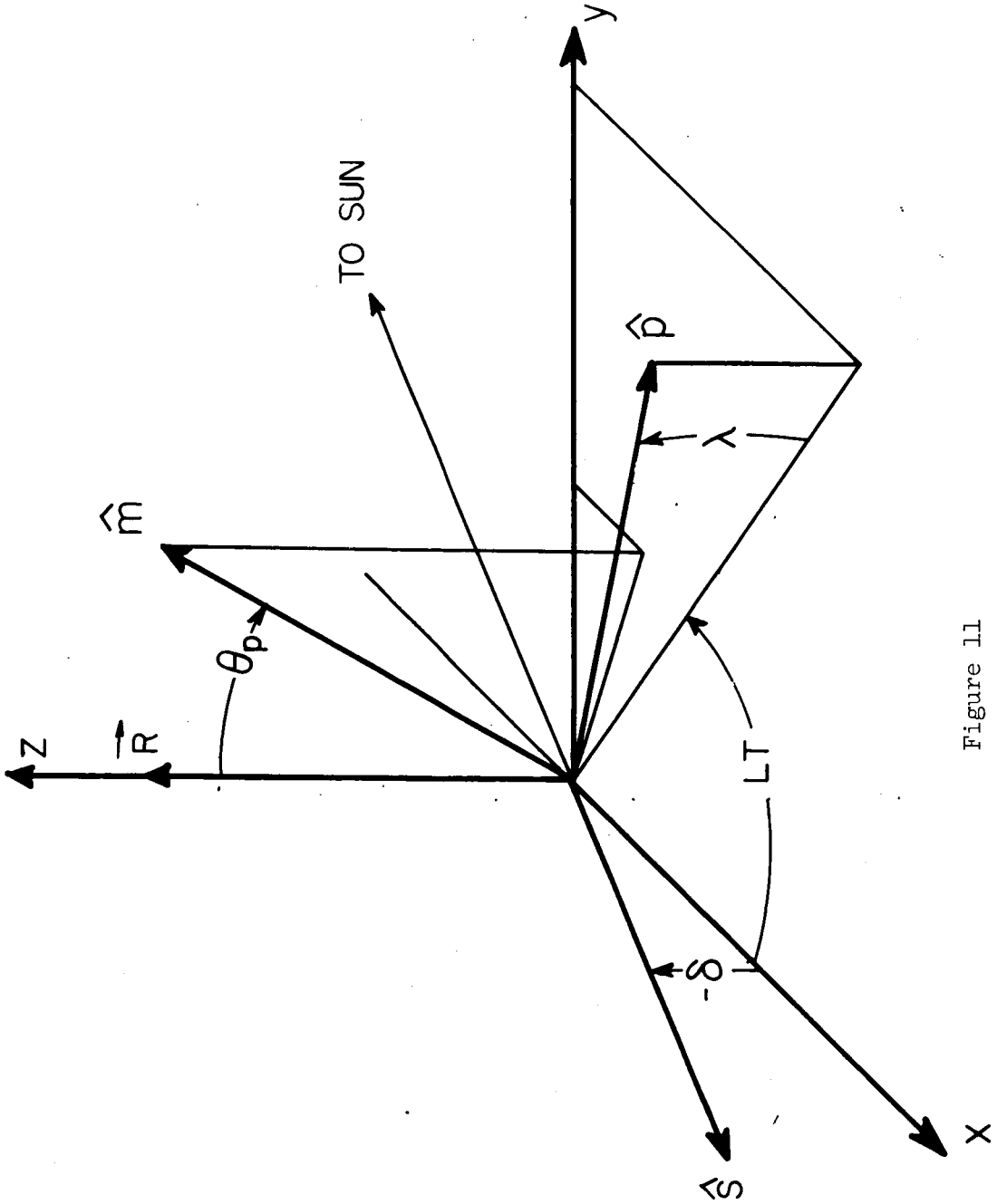


Figure 11

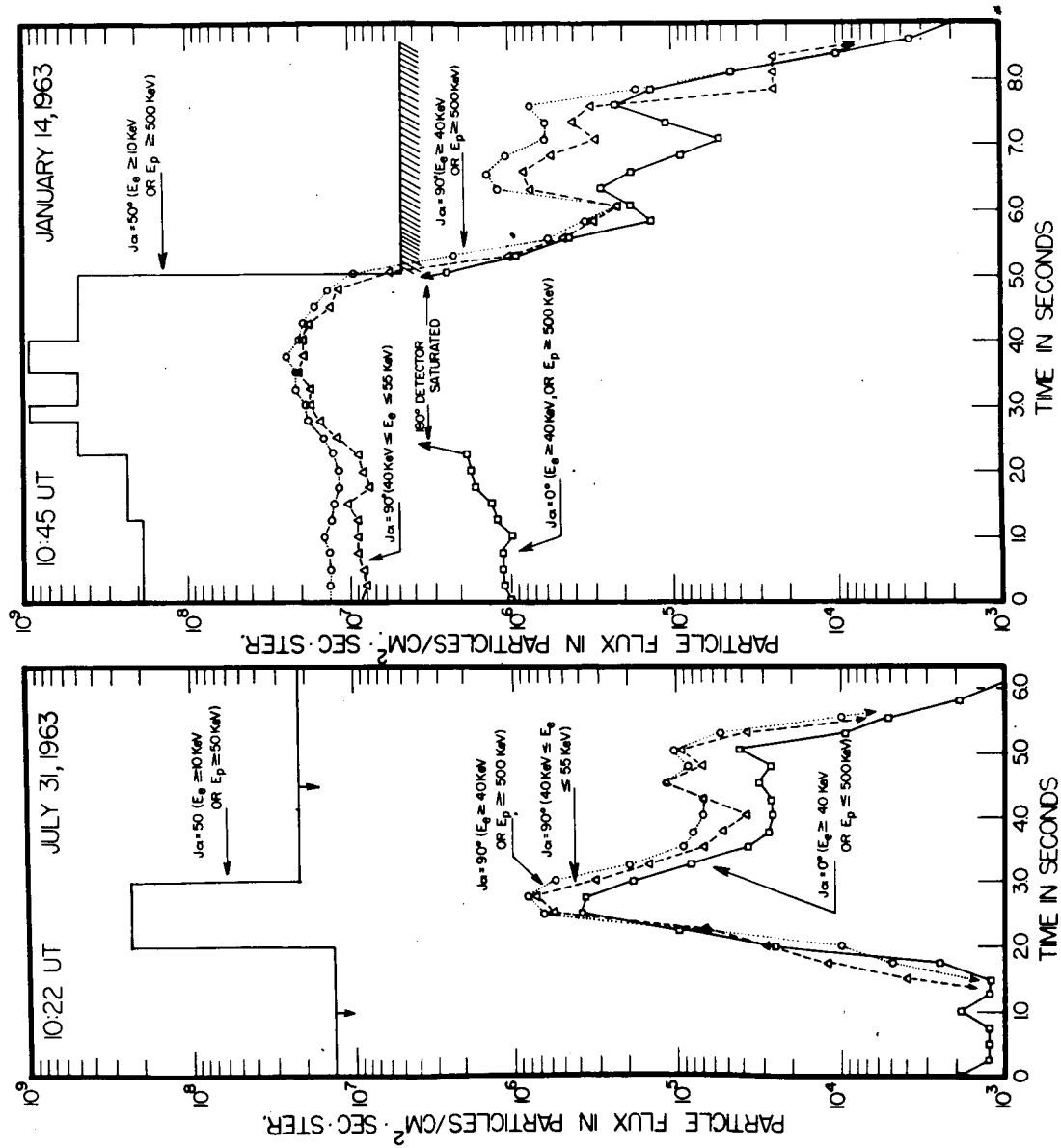


Figure 12